Marine Pollution Bulletin 201 (2024) 116225

Contents lists available at ScienceDirect

Marine Pollution Bulletin

journal homepage: www.elsevier.com/locate/marpolbul

# Sedimentary environmental quality of a biosphere reserve estuary in southwestern Iberian Peninsula

A. Barba-Lobo [a,b,*], B. García-González [a], J.L. Guerrero [a,c], J.P. Bolívar [a]

[a] Radiation Physics and Environment Group (FRYMA), Department of Integrated Sciences, Center for Natural Resources, Health and Environment (RENSMA), University of Huelva, 21007 Huelva, Spain
[b] Department of Medical Radiation Sciences, Institute of Clinical Sciences, Sahlgrenska Academy at University of Gothenburg, Gothenburg SE-413 45, Sweden
[c] Department of Biology and Geology, Physics and Inorganic Chemistry, Higher School of Experimental Sciences and Technology, Rey Juan Carlos University, c/Tulipán s/n, 28933 Móstoles, Spain

ARTICLE INFO

*Keywords:*
Phosphogypsum piles
Fertilizer industry
Acid mine drainage
Trace elements
Natural radionuclides
Pollution indexes

ABSTRACT

The Huelva estuary is formed by the common mouths of the Odiel and Tinto Rivers, and inside this ecosystem is the biosphere reserve of the Odiel saltmarshes. This ecosystem has been historically affected by acid mine drainage (AMD) and by releases of pollutants from five phosphoric acid industrial plants and phosphogypsum (PG) waste stacks located in the area. This study carried out a comprehensive assessment of the environmental impact of the biosphere reserve of the Odiel saltmarshes. To this end, it was necessary to find a suitable sedimentary background (Piedras River in our case). To quantify this impact, several pollution indexes were used. According to the values reached by the indexes, this impact was classified as "serious" pollution for most trace elements, excepting the deepest layers, and "low-moderate" pollution for the $^{238}$U-series radionuclides, while no pollution for the $^{232}$Th-series and $^{40}$K radionuclides was found as expected.

## 1. Introduction

The estuary of Huelva is in Southwestern Spain, and it is formed by the common mouths of the Tinto and Odiel Rivers (see Fig. 1), which among of the most polluted rivers in the world by acid mine drainage (AMD). Their waters contain very high levels (3–5 orders of magnitude higher than unperturbed surface waters) of heavy metals and natural radionuclides, especially for U and Th isotopes (Olías et al., 2006; Nieto et al., 2007; Nieto et al., 2013; Guerrero et al., 2021a). In addition, a very large industrial chemical complex is located in this estuary, whose activity began in 1965, including plants devoted to the production of fertilizers, ammonia, copper by smelting/electrorefining, oil refining, petrochemical, $TiO_2$ pigments, etc. Both pollution sources (mining and industry) have produced a high historical pollution of this estuary from the XIX century to the present day (Borrego et al., 2002; Morillo et al., 2004; Pérez-López et al., 2011).

A large fraction of the basins of these rivers is in the Iberian pyrite belt (IPB), southwest of the Iberian Peninsula, which is one of the major deposits of massive polymetallic sulphurs in the world, with an estimated polymetallic sulphur reserve of about 1.7 Gt (Sáez et al., 1999). These deposits were mined by previous civilizations such as Tartessos and Roman, although the greatest mining activity started in the second half of XIX century, mainly by British and French mining companies, generating old mining galleries, millings, and several types of waste in the north of the Huelva province (Mujica et al., 2008). These "legacy sites" contain the sources of the AMD problem in both Odiel and Tinto Rivers waters, since the basins of these rivers receive waters from the IPB.

AMD is produced by the oxidation of these residual materials that interact with the water and its dissolved oxygen, generating the release of $Fe^{2+}$ and a great acidification of the aqueous medium reaching pH values of 1–2 (Aduvire, 2006). These sulphurs are mainly composed of iron pyrite ($FeS_2$), and variable proportions of other subordinate minerals such as sphalerite (ZnS), galena (PbS), chalcopyrite ($CuFeS_2$), arsenopyrite (FeAsS), pyrrhotite ($Fe_{1-x}S$), and many other minor phases, such as Bi- and Pb-sulfosalts, cassiterite, magnetite, stannite, electrum and cobaltite. As a result of the AMD process, those minor elements contained in the sulphur minerals and their host-rocks are released into the aqueous matrix (heavy metals, rare earth elements, radionuclides, *etc.*), generating very polluted waters (Curcio et al., 2019).

* Corresponding author at: Radiation Physics and Environment Group (FRYMA), Department of Integrated Sciences, Center for Natural Resources, Health and Environment (RENSMA), University of Huelva, 21007 Huelva, Spain.
*E-mail addresses:* alejandro.barba@dci.uhu.es, alejandro.barba-lobo@gu.se (A. Barba-Lobo).

https://doi.org/10.1016/j.marpolbul.2024.116225
Received 28 October 2023; Received in revised form 26 February 2024; Accepted 2 March 2024
Available online 8 March 2024

Another pollution problem in the Huelva estuary is related to the chemical industrial complex located in its vicinity, whose plants have released very large amounts of pollutants, mainly heavy metals, natural radionuclides and anions into the Huelva estuary. In relation to the phosphoric acid production, five production plants were installed in the estuarine zone, using phosphate rock (PR) from Morocco as main raw material. The Moroccan phosphate rock is characterized by having a high concentration of $^{238}$U (around 1500 Bq kg$^{-1}$, equivalent to about 50 ppm of natural U), which is about 50 times higher than the concentration of $^{238}$U in non-polluted soils (UNSCEAR, 2000). During the process, a by-product called phosphogypsum (PG) is generated, containing over 95 % of radioactivity initially contained in the raw material ($^{226}$Ra, $^{230}$Th and $^{210}$Pb), but only about 10–20 % of $^{238}$U from the raw material (Bolívar et al., 2009; Gázquez et al., 2009).

Three different periods are distinguished management of PG in Huelva. The first period was between 1965 and 1997, when 20% of the PG was discharged directly into the Odiel channel, while the remaining 80% was transported using estuarine water and deposited in piles in the right shore of the Tinto River channel; while the water used in the transport, with a pH around 1.5 and high concentration of metals and radionuclides, was returned into the Tinto River (Bolívar et al., 1995; García-Tenorio and García-León, 1996; Bolívar et al., 2008; Gázquez et al., 2009). During the second period (1998 to the end of 2010), all the PG generated in the five phosphoric acid (PA) factories using freshwater in a closed circuit, since the used water was pumped back into the factories to be employed again for PG pumping. Lastly, on December 31st, 2010, the PA production was stopped and, since then, there has been no generation of PG in Huelva (Hierro et al., 2012).

The main problem related to the direct discharges of PG into the Odiel channel, and to a lesser extent the leachates from PG waste piles, are the releases of a large number of natural radionuclides such as $^{238}$U, $^{226}$Ra, $^{210}$Pb or $^{210}$Po, and toxic elements like Fe, Zn, As, Cr or Cd to their surroundings (Pérez-López et al., 2016; Papaslioti et al., 2018; Guerrero et al., 2021a, 2021b). Nowadays there are around 100 Mt. of phosphogypsum distributed along 1000 ha on the western shore of the Tinto River, divided into 4 different areas (Hierro et al., 2013).


**Fig. 1.** Study area selected for the samplings carried out in this work. The sediment cores were taken from Piedras River and Bacuta Island.

For these reasons, that is, due to both AMD releases and phosphogypsum leachates (PGL), the estuary of Huelva has a significant pollution level, which is caused by releases of trace elements and natural radionuclides. This can be corroborated by other studies on the pollution in the Odiel and Tinto Rivers (Borrego et al., 2002; Pérez-López et al., 2011).

Consequently, the aim of this study was to assess and update the environmental impact on the Odiel River estuarine biosphere reserve, for which vertical profiles were analyzed. Furthermore, different pollution indexes were obtained in order to assess the environmental impact, which was possible due to the proper selection of a sedimentary background, also called baseline, that must be geochemically similar to the analyzed problem sedimentary system (Le Gall et al., 2018; Luo et al., 2022).

Considering all of the above mentioned, to the best of our knowledge, this is the most updated study about the environmental impact on the estuarine biosphere reserve in the Southwestern Iberian Peninsula. In addition, an exhaustive assessment and establishment of a proper sedimentary background (Piedras River in our case) was carried out, which was then compared with several sedimentary backgrounds placed at Southwestern Iberian Peninsula. Moreover, the impact in Bacuta Island was carefully quantified using several pollution and toxicity indexes for major and trace elements, heavy metals and natural radionuclides, where the different pollution sources were identified using correlation analysis. Furthermore, the procedure followed in this study to select a suitable sedimentary background, assess the environmental impact in the sedimentary system of interest and identify the different pollution sources can be applied to any sedimentary system worldwide.

## 2. Materials and methods

### 2.1. Sampling

Samplings were carried out in November 2021, taking a sediment core from Bacuta Island in the biosphere reserve of the Odiel saltmarshes and another one from the Piedras River, using this latter as sedimentary reference system to assess the background of this geographical area. This was necessary, as its geochemical substrate must be similar to that of the Huelva estuary and contain no detectable influence from AMD, PG stacks or the chemical complex (see Fig. 1). Every core was 60 cm deep and was cut into 2 cm thick sections (Fig. A.1, in Supplementary Material – Appendix A). Then, the 2 cm thick samples were dried in an oven at 60 °C until constant weight, grinded by agate mortar, and finally homogenized.

### 2.2. Characterization techniques

The major elements were analyzed by X-ray fluorescence (XRF) using a Panalytical Spectrometer AXIOS instrument at the Research, Technology and Innovation Center of the University of Seville (CITIUS). Trace elements were analyzed by inductively coupled plasma mass spectrometry (ICP-MS) at Activation Laboratories (Actlabs, Ontario, Canada), for which the samples were previously digested with strong acids such as hydrofluoric acid, followed by a mixture of nitric acid and perchloric acid. A granulometric analysis was carried out by laser diffraction, using a Malvern Mastersizer 2000 instrument at the General Services of the University of Huelva. The radionuclides by gamma-ray spectrometry were determined using a Well-type high purity germanium (HPGe) detector and an extended range HPGe detector (XtRa), whose efficiency calibrations were developed by Barba-Lobo et al. (2021a) and Barba-Lobo et al. (2021b), respectively. This technique is widely used by the Radiation Physics and Environment Research Group (FRYMA) of the University of Huelva.

### 2.3. Quality control

All the measurements that were not carried out by the research group FRYMA, were ordered to accredited external laboratories. For every measurement, one replica and one blank per every ten samples were included, as well as certificated reference materials (CRMs) provided by the IAEA (International Atomic Energy Agency), where two CRMs were of soil type (IAEA-326 and IAEA-327) and another of phosphogypsum type (IAEA-434), obtaining $z_{score}$ values generally below 2. In addition, the laboratory of the FRYMA group annually participates in several intercomparison exercises, where gamma-ray spectrometry was employed for the analysis. To guarantee the reliability of the results, many different comparisons between different analysis techniques were conducted, such as the comparison between ICP-MS and gamma-ray spectrometry. The detection limits obtained for ICP-MS and gamma-ray spectrometry ranged from 0.05 ppm to 0.1 ppm, and from 2 Bq $kg^{-1}$ to 20 Bq $kg^{-1}$, respectively.

In addition, the validation for gamma-ray spectrometry was also accomplished by comparing the $^{40}K$ concentration obtained by using gamma-ray spectrometry with that concentration obtained by means of XRF using the relationship: 1 % of natural K → 313 mBq/g of $^{40}K$ (Barba-Lobo et al., 2021a).

### 2.4. Pollution and toxicity indexes

To evaluate the environmental impact of AMD and phosphogypsum discharges on the Huelva estuary, several pollution indexes were used. The classification for every pollution index is shown in Table A.1 (Supplementary Material – Appendix A).

#### 2.4.1. Enrichment factor (EF)

The enrichment factor for an element (i) in a sample (s), $EF_i$, was used to evaluate the degree of anthropic pollution in soils and sediments using a conservative element as normalizer of concentrations, with Al being the most used (Díaz-Asencio et al., 2011; Hakason, 1979; Lario et al., 2016; Zhang et al., 2016). *EF* can be calculated using Eq. 1:

$$EF_i = \frac{\left(C_i/C_{Al}\right)_s}{\left(C_i/C_{Al}\right)_r} \quad (1)$$

where $C_i$ is the concentration of a specific element (i) in the sample (s), $(C_i)_s$, and in the reference (r), $(C_i)_r$, and $C_{Al}$ is the concentration of Al in the sample, $(C_{Al})_s$, and in the reference, $(C_{Al})_r$.

#### 2.4.2. Contamination factor (CF)

To estimate the pollution level of a specific element with respect to a typical soil, the contamination factor, *CF*, is calculated using the following equation (Gözel et al., 2022; Vineethkumar et al., 2020):

$$CF_i = \frac{(C_i)_s}{(C_i)_r} \quad (2)$$

where $(C_i)_s$ is the concentration of an element (i) present in the sample (s) and $(C_i)_r$ is referred to the concentration of this element reference (r) system, which in our case was taken from (Rudnick and Gao, 2003).

For *CF* assessment in the case of natural radionuclides, that is, $^{238}U$-series, $^{232}Th$-series and $^{40}K$, the activity concentrations stablished by UNSCEAR (2000) for unpolluted typical soils, that is, 35 Bq $kg^{-1}$, 30 Bq $kg^{-1}$ and 400 Bq $kg^{-1}$ for $^{238}U$, $^{232}Th$ and $^{40}K$, respectively, were used as reference activity concentrations.

#### 2.4.3. Contamination degree (CD)

The contamination degree (*CD*) is a factor to measure the mean level of contamination of a sample/material by considering all the toxic elements, such as As, Cd, Cr, Cu, Ni, Pb and Zn, and it can be calculated

using the following equation (Vineethkumar et al., 2020; Yushin et al., 2023):

$$CD = \frac{\sum_{i=1}^{n} FC_i}{n} \quad (3)$$

where $n$ is the number of elements (i) considered for the $CD$ calculation.

#### 2.4.4. Potential ecological risk (PER)

The potential ecological risk ($PER$) is a factor by which it is possible to assess the toxicity associated with the presence of heavy metals (Kerolli-Mustafa et al., 2015; Liu et al., 2021), that is, Cd, Cr, Cu, Ni, Pb and Zn, as well as As (metalloid) (a total of seven elements). The $PER$ for an element "i" is calculated using the following equation:

$$PER_i = CF_i \cdot T_i \quad (4)$$

where $CF_i$ is the contamination factor of the element (i), and $T_i$ is the toxicity factor for this element, that is, $T_i$ is based on the principle of abundance, which indicates that the potential toxicological effect of an element is proportional to its abundance, or rarity, in nature. $T_i$ has a specific value for each heavy metal and As (Kerolli-Mustafa et al., 2015; Liu et al., 2021).

#### 2.4.5. Potential toxicity of a sample (PT)

Regarding the potential risk that a sample or material can produce, the potential toxicity index ($PT$) is calculated as follows (Kerolli-Mustafa et al., 2015):

$$PT = \sum_i PER_i \quad (5)$$

### 2.5. Data treatment

In the case of the data treatment, a principal component analysis (PCA) was performed providing the data interpretation, using XLSTAT software (Lumivero, 2023). Firstly, the correlation matrix of the variables was calculated, starting from the matrix of original data. Then, the calculation of the factor matrix, starting from the Pearson's "r" of the previous matrix.

## 3. Results and discussion

For the cores taken from the Piedras River and Bacuta Island, a granulometric analysis was conducted to evaluate the pollutant sorption capacity of the samples, and concentrations of stable elements (major and trace elements) were measured. Then, the suitability of the Piedras River as a sedimentary background was tested, and the environmental impact in Bacuta Island was assessed. Finally, a correlation analysis was carried out for the Piedras River and Bacuta Island to determine the influence of the pollution sources on both sedimentary systems.

### 3.1. Baseline for estuaries from the Southwest of Spain

#### 3.1.1. Granulometry

The granulometric analysis is very useful for the generation of information on the predominant grain size of each sedimentary systems and, therefore, the predominant specific surface area of the grains present in the samples, with pollutant sorption increasing as the grain size decreases.

The granulometry distribution is very similar for most of the core samples, and an example of this distribution (depth = 16 cm, Piedras River) is shown in Fig. A.2a (Supplementary Material – Appendix A). Thus, a maximum value was observed at about 10 μm, which suggests that a fine fraction is predominant, with the fine fraction (clay + silt) representing about 80% of the samples. However, another two small relative maximum values were detected at about 300 μm and 500 μm, which suggests that coarse fractions are also present, especially in the deepest samples (52 cm), with about 40% of sand.

Fig. A.2b presents the percentages of the different granulometric fractions obtained for the five selected samples of the core (depths = 2 cm, 16 cm, 30 cm and 52 cm) analyzed by laser diffraction in the case of the core taken from the Piedras River. As can be observed in Fig. A.2b, the silt fraction ranged from 54% (depth = 52 cm) to 88% (depth = 16 cm). However, a significant presence of the different types of sand was also identified, which is especially true for fine and medium sands, ranging from 3% (16 cm) to 29% (52 cm), and from 1% (16 cm) to 14% (52 cm), respectively. In addition, at 2 cm of depth, there was a significant contribution of coarse sand which was found to be about 10%.

Consequently, according to the results shown in Fig. A.2, it is possible to state that the presence of the coarse fraction is relatively significant for all the samples, except for depth = 16 cm.

#### 3.1.2. Concentrations of major and trace elements

The concentrations of the major and trace elements were obtained for the different depths analyzed for the core taken from the Piedras River. As can be seen in Fig. 2, the concentrations obtained for the major elements were similar to those found in typical soils (Rudnick and Gao, 2003), where the concentrations of K, Na and Mg (Fig. 2a) ranged from 1% to 2%, which are concentrations for typical soils. This is consistent with the granulometric analysis (see Fig. A.2), where the coarse fraction (fine sand + medium sand + coarse sand) was relatively high, that is, the $SiO_2$ content must also be relatively high, as was the case for the Piedras River core. With regard to Fe and S (Fig. 2b), their concentrations ranged from 2% (52 cm) to 4.5% (30 cm), and from 0.3% (42 cm) to 1.8% (30 cm), respectively, which are slightly higher than those of typical soils. This is consistent, since the Piedras River basin contains some areas belonging to the Iberian pyrite belt (IPB), which is characterized by the presence of massive polymetallic sulphurs. Furthermore, Fig. 2b also shows that the concentration of Al is relatively low at the deepest layers (e.g., 52 cm). This agrees well with the granulometric fractions obtained at 52 cm of depth, where contributions of fine and medium sands were higher than those found for a typical soil. Therefore, the percentage of $SiO_2$ present at that depth was also higher than that found for a typical soil, indicating that the Al concentration was lower than that in a typical soil. In regard with Ti and P (Fig. 2c), no significant concentrations were found (below 0.8% and 0.05%, respectively) in any of the analyzed depths. In addition, for most of the major elements, two maximum values (8 cm and 30 cm of depth) were observed, which must correspond to a natural enrichment.

Regarding trace elements (Fig. 2d, e and f), their concentrations were generally at the same order of magnitude as those found in unperturbed sediments, which is in agreement with the results obtained with major elements and granulometric fractions. There were only two exceptions, Cu and Zn, whose concentrations ranged from 100 μg $g^{-1}$ to 350 μg $g^{-1}$, and 100 μg $g^{-1}$ to 600 μg $g^{-1}$, respectively. However, this is consistent with the geographical location of the Piedras River, which is located near the IPB, where massive polymetallic sulphurs are present. In addition, for most the trace elements, two maximum values were also found for the same depths as those observed for major elements, which is consistent.

#### 3.1.3. Concentrations of natural radionuclides

In the case of the concentrations obtained for natural radionuclides ($^{238}$U-series, $^{232}$Th-series and $^{40}$K) at the different depths considered for the core taken from the Piedras River, these are shown in Fig. 3. As can be seen in Fig. 3a, the concentrations of the different radionuclides belonging to the $^{238}$U-series ($^{238}$U, $^{226}$Ra and $^{210}$Pb) ranged from 21 Bq $kg^{-1}$ to 46 Bq $kg^{-1}$, from 16 Bq $kg^{-1}$ to 27 Bq $kg^{-1}$, and from 17 Bq $kg^{-1}$ to 41 Bq $kg^{-1}$, respectively. These concentrations are in line with those found for typical soils (UNSCEAR, 2000). For $^{232}$Th-series ($^{228}$Ra and $^{228}$Th) and $^{40}$K (Fig. 3b), activity concentrations (20–37 Bq $kg^{-1}$, 24–40 Bq $kg^{-1}$ and 373–789 Bq $kg^{-1}$ for $^{228}$Ra, $^{228}$Th and $^{40}$K, respectively)

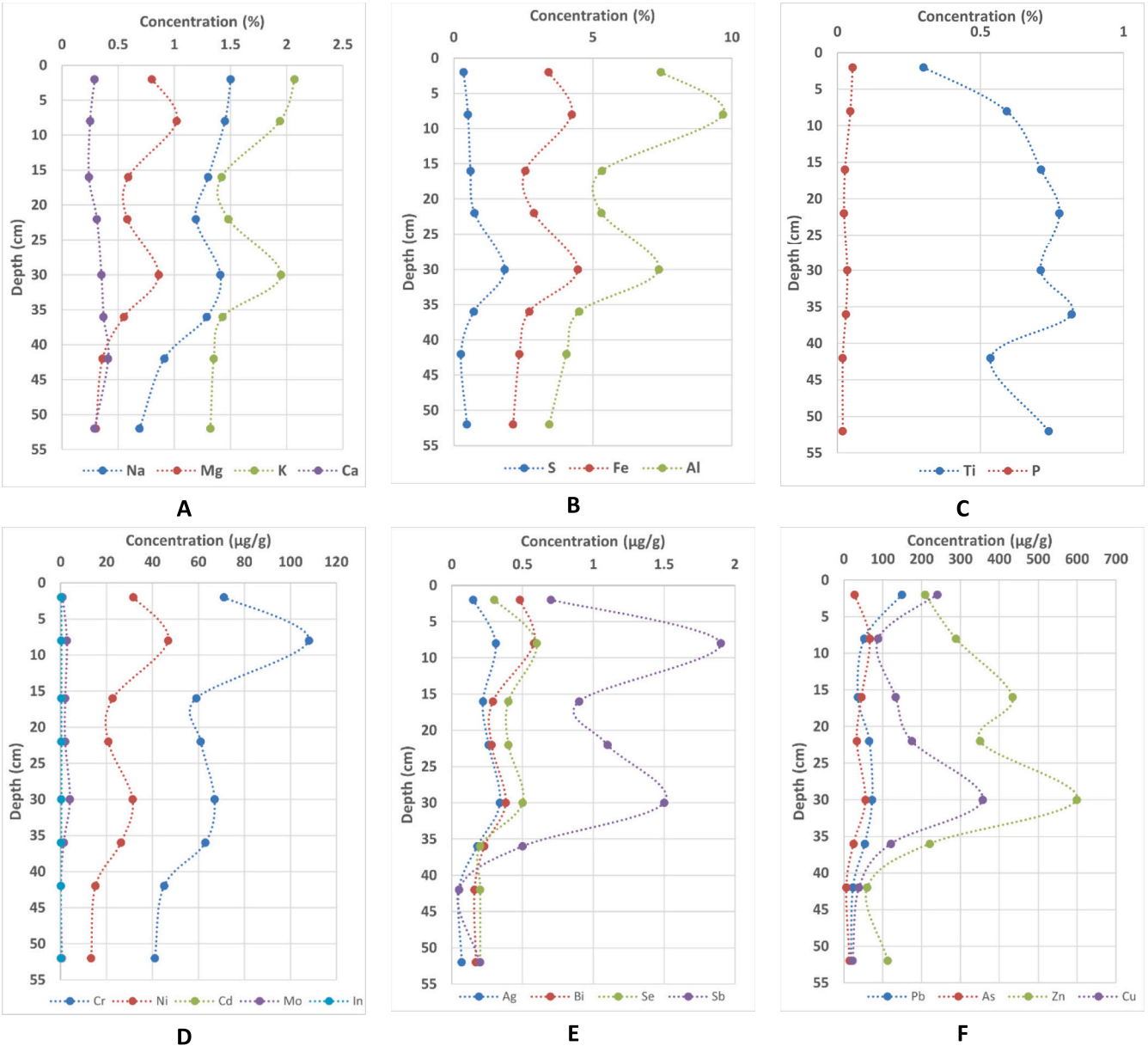


**Fig. 2.** Concentrations of both major (from A to C) and trace (from D to F) elements contained in the core taken from the Piedras estuary.

were also found to be very similar to those present in typical soils. This is very consistent with the concentrations obtained for stable elements (see Fig. 2) and granulometric fractions (see Fig. A.2). Furthermore, Fig. 3 shows maximum concentrations at about 8 cm and 30 cm, which is in agreement with those maximum concentrations found for stable elements.

### 3.1.4. Background assessment

To decide whether the Piedras River can be considered as a proper sedimentary background (baseline), it is necessary to assess different types of pollution indexes (such as *EF* and *CF*) for stable elements and radionuclides. To this end, it is necessary to use the concentrations of the stable elements (heavy metals in this study) and radionuclides.

The enrichment factor, *EF*, was calculated for heavy metals and As. The *EFs* obtained in our case were compared with those resulting from other sedimentary systems present in geographical regions close to the study area, selecting the estuaries of Formosa, Guadiana, Odiel and Guadalquivir for comparisons with our reference area (Piedras estuary). The Piedras River was selected based on the fact that previous works (Caliani et al., 1997; Lario et al., 2016) have demonstrated that no mining activities have been developed on its basin. In addition, for these sedimentary systems, the data provided by Rudnick and Gao (2003) for the mean of the upper earth crust were used as reference, and Al was considered as the normalizer element due to its conservative behavior (Zhang et al., 2016; Lee et al., 2021). The *EFs* for heavy metals and As are shown for the different sedimentary systems in Fig. 4. In our case, we distinguished two cases for our studied core, that is, Piedras-2 (two deepest samples) and Piedras-3 (entire core).

As can be seen in Fig. 4, *EF* was calculated according to Rudnick and Gao (2003) for different estuary systems. The *EFs* obtained for great majority of the stable elements were below 2. This result demonstrates that there is no significant pollution for any of them, with similar *EF* values being found in all cases. This is especially true in the comparison between our case (Piedras-2 and Piedras-3) and Piedras-1 (Lario et al., 2016), since the Piedras-1 core was collected from a region very close to that corresponding to the core selected for our study. Furthermore, in the case of Piedras-2, lower *EFs* were achieved compared with those resulting from Piedras-3. Therefore, the Piedras River is a proper

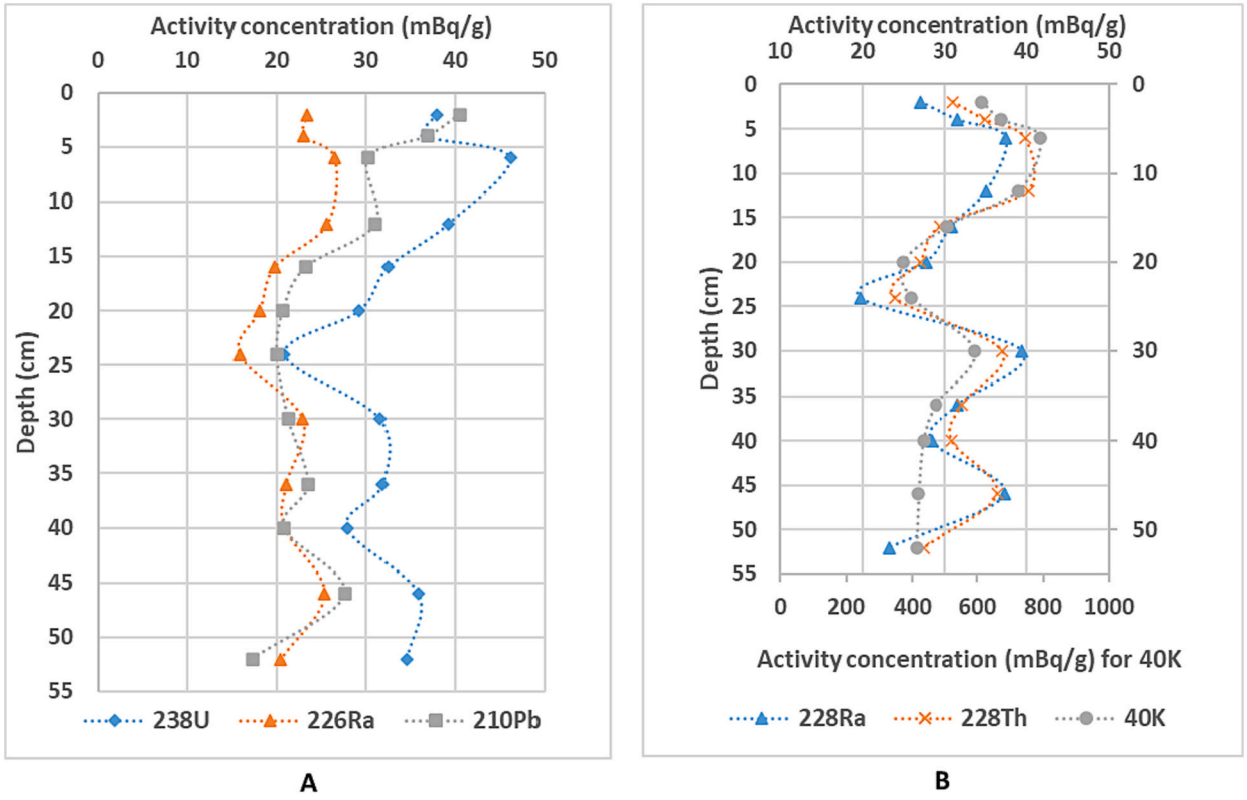


**Fig. 3.** Concentrations of radionuclides, belonging to the $^{238}$U-series (A), and to the $^{232}$Th-series and $^{40}$K (B), present in the core taken from the Piedras estuary.

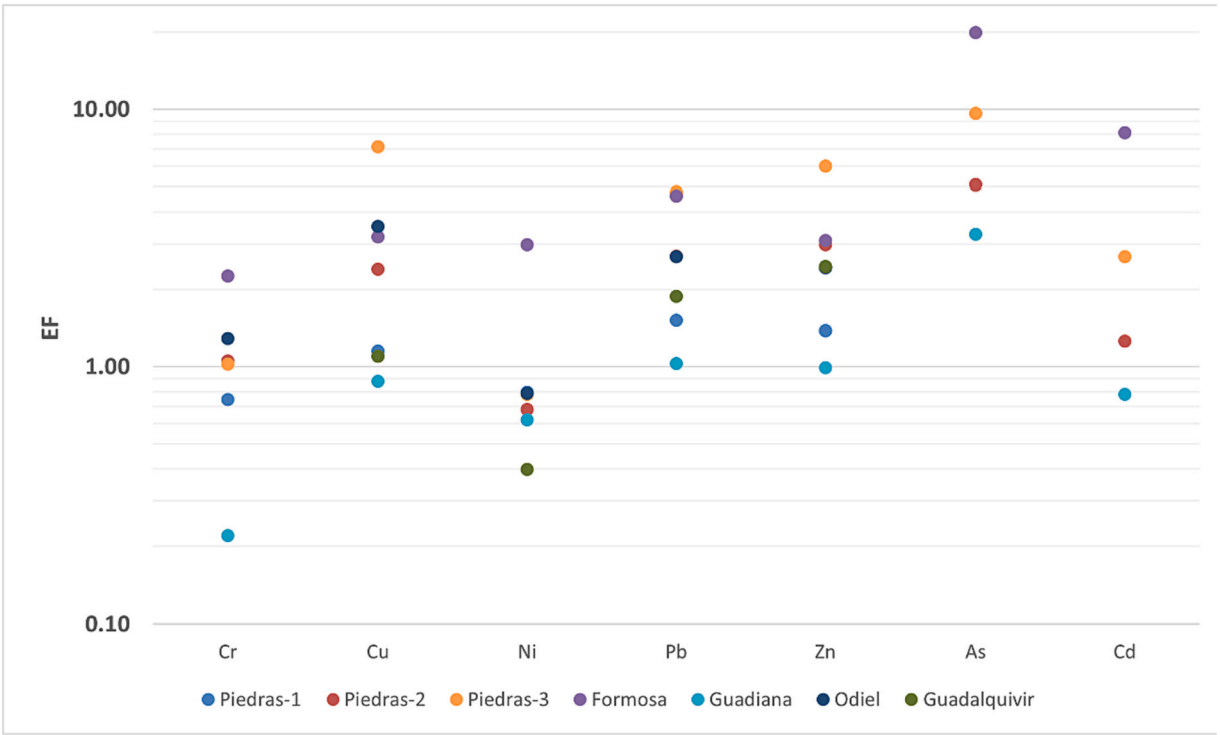


**Fig. 4.** Enrichment factors (*EF*) calculated according to Rudnick and Gao (2003) for different estuary systems. Piedras-1: Deep core (several meters) of Piedras estuary (Lario et al., 2016); Piedras-2: Core of Piedras estuary, considering the two deepest samples (this study); Piedras-3: Core of Piedras estuary, considering the entire core (this study); Formosa: Surface samples from Formosa estuary (Sousa et al., 2019); Guadiana: Surface samples from Guadiana estuary (Delgado et al., 2012); Odiel: Surface samples from Odiel estuary (Borrego et al., 2002); Guadalquivir: Surface samples from Guadalquivir estuary (Riba et al., 2002).

background, with Piedras-2 (average between the two deepest samples) being a more appropriate option, although the concentrations of all elements is not known; therefore, we took the element concentrations of our study as baseline (background) for the estuaries located in Southwestern Spain.

In the case of the natural radionuclides ($^{238}$U, $^{228}$Ra, $^{228}$Th and $^{40}$K), *EF* and *CF* were calculated for the entire core, i.e., 12 samples (see Fig. A.3 in Supplementary Material – Appendix A). As can be seen in Fig. A.3a, the *EF* values were generally between 1 and 2; therefore, according to Table A.1, no significant pollution due to radioactivity was found. For further corroboration, *CF* was also obtained for the same radionuclides and depths, achieving *CF* values of 1.5 in most cases (Fig. A.3b). Consequently, it is possible to conclude that the Piedras River is a proper background in our case for natural radionuclides in estuarine sediments from this geographical area.

In addition, to establish a proper baseline, numerical information of the concentrations of all the stable elements and radionuclides measured was included. In Table A.2 (see Supplementary Material – Appendix A), concentrations of major elements and radionuclides for all the depths considered for this core can be consulted, as well as their average values and their respective standard deviations (SD) and standard deviations of the average (SU). Analogously to Table A.2, Table A.3 (see Supplementary Material – Appendix A) shows numerical information about the concentrations of trace elements for all the considered depths, as well as their average values. Thus, Table 1 shows the concentrations of major elements, natural radionuclides and trace elements established as background values for the Piedras estuary core analyzed in this study. For this, the average between the two deepest samples of the Piedras estuary core was considered (that is, Piedras-2 in Fig. 4) since it is a more appropriate option as sedimentary background, as previously demonstrated. In addition, the sedimentation rate of the Piedras core analyzed in this study was obtained by the $^{210}$Pb dating method (San Miguel et al., 2001), which was about 0.25 cm yr$^{-1}$, showing that the age of its two deepest layers (42 cm and 52 cm) is about 170 and 210 years, respectively, that is, before the beginning of the Second Industrial Revolution. Consequently, since no pollution source was found for those sediment ages, this further corroborates that the sedimentary background was properly established using the Piedras River core analyzed in this study.

At a national level, the Spanish Royal Decree 9/2005 establishes that the guideline levels for contaminated soils that require remediation measurements are those with heavy metal concentrations over 100 times the baseline values (Royal Decree, 2005). No studies have been carried out to assess the base line of the estuaries located in Southwestern Spain for major elements, trace elements, metalloids and rare earth elements. Therefore, additional analyses (described in the next section) were carried out to further verify that the Piedras River core used in this work showed no impact.

#### 3.1.5. Correlation analysis and pollution sources

To find possible contributions of the different potential pollution sources existing in this geographical area (AMD, industries, wastewater releases, *etc.*), a correlation analysis was conducted between the different stable elements. The criterion followed for the selection of these elements was the one that allows obtaining a significant correlation coefficient, in this case $R > 0.8$, for a significance level of 0.05. The Spearman's correlation matrix in Supplementary Material – Appendix B was included, as well as the plots of the most relevant correlations in Fig. A.4 (see Supplementary Material – Appendix A).

As can be seen in Fig. A.4, the correlation between Mg and Fe was positive. In the case of the Piedras River, Mg is a naturally occurring element. This suggests that, for the Piedras River, an enrichment of Fe is also naturally occurring, which is consistent, given that the Piedras River is not significantly affected by pollution sources, as proven in Sections 3.1.2 to 3.1.4, with the existence of only natural enrichments, due to the mixing of seawaters with the fluvial ones. Th and Fe, showed a similar behavior, that is, a positive correlation. Therefore, this suggests that Th is naturally enriched, since Fe was proven not to be contributed by any pollution source in the case of the Piedras River. Then, for the As—Fe pair, a positive relationship was also observed, which is consistent, given that the Piedras River is located near the Iberian pyrite belt. Therefore, As is naturally present, due to the massive polymetallic sulphurs. Fe was selected for these three cases based on the fact that it is the tracer of the pollution coming from AMD. Consequently, no impact generated by AMD was found in the case of the Piedras River.

As has been demonstrated in previous studies (Bolívar et al., 2009), the P element is a very good marker of the pollution coming from fertilizer industry releases. Thus, in Fig. A.4, U, Bi and Pb were plotted against P, achieving positive correlations for the three cases. This means that U, Bi and Pb are naturally enriched, since the Piedras River is not affected by PGL.

It is interesting to highlight that the correlation between Fe and P was also relatively high ($R = 0.71$, see Supplementary Material – Appendix B), which can be explained by the fact that both elements are naturally enriched; therefore, both have similar origin in the case of the Piedras River.

### 3.2. Odiel estuary

Once the background was established and its suitability was proven, we then assessed the environmental impact in the Odiel River channel. To this end, an order analogous to Section 3.1 was followed when applying the different analysis techniques.

#### 3.2.1. Granulometry

As can be seen in Fig. A.5a (see Supplementary Material – Appendix A), an example of granulometric curve (depth = 42 cm) was shown for the core taken from the Bacuta Island. Thus, a maximum grain size slightly higher than 10 μm was found, which proves the predominance of the fine fraction (silt in this case). Another maximum at about 1000 μm was also observed, which is related to the coarse fraction (coarse sand in this case), but its contribution can be neglected comparing it with that found for the fine fraction.

In the case of Fig. A.5b, two fractions were clearly predominant: silt and fine sand. For silt and fine sand, the granulometric fractions ranged from 61 % (depth = 2 cm) to 84 % (depth = 42 cm) and from 8 % (depth = 42 cm) to 22 % (depth = 2 cm), respectively. For all the other granulometric fractions, their respective percentages were below 5 % for most cases. The relatively high percentage of fine fraction at 42 cm of

**Table 1**
Concentrations of major elements (in %), natural radionuclides (in Bq kg$^{-1}$) and trace elements (in μg g$^{-1}$) established as background values for the Piedras estuary core analyzed in this study.

| Na | Mg | Al | K | Ca | Fe | Ti | P | S | $^{226}$Ra | $^{232}$Th | $^{40}$K |
|---|---|---|---|---|---|---|---|---|---|---|---|
| 0.80 | 0.33 | 3.74 | 1.34 | 0.35 | 2.25 | 0.64 | 0.018 | 0.37 | 20.8 | 27.4 | 442 |

| Cd | Cr | Ni | Ag | Bi | Se | Zn | As | Mo | In | Sb | Cu | Pb |
|---|---|---|---|---|---|---|---|---|---|---|---|---|
| <0.1 | 43 | 14 | 0.06 | 0.17 | 0.20 | 87 | 11 | 0.36 | <0.1 | 0.13 | 21 | 31 |

depth (almost 90 % considering silt + clay) suggests that it is very likely to find a maximum of concentrations of the different pollutants (trace elements and radionuclides) at about that depth.

### 3.2.2. Concentrations of major and trace elements

As can be seen in Fig. 5, the concentrations of major elements (Fig. 5a, b and c) and trace elements (Fig. 5d, e and f) were shown for the different depths considered in the case of the core taken from Bacuta Island, having selected the same stable elements as those analyzed for the Piedras River (see Fig. 2 in Section 3.1.2). In addition, the concentrations of major elements and trace elements can be consulted in Tables A.4 and A.5, respectively (Supplementary Material – Appendix A).

Na, Mg, K and Ca (Fig. 5a) showed similar behaviors as those found for the Piedras River (see Fig. 2a), that is, they were relatively stable along all the sediment core, and the concentrations of all these elements were very similar for both sedimentary systems along all vertical profiles. This is consistent, since these are naturally present in both sedimentary systems. For Na, it is possible to observe a slight increase at superficial layers, which could be due to the contribution of seawater contained in the pores of the sediments. In the case of Fe and S (Fig. 5b), their concentrations were relatively higher than those found for the Piedras River (see Fig. 2b), that is, about 2–7 times and 2–6 times higher, respectively. These relatively high concentrations can be due to the significant affection of AMD in Bacuta Island, where Fe can be used as a tracer of AMD influence. Fig. 5c shows very similar behaviors and concentrations for Ti compared with the core taken from Piedras River (see Fig. 2c). This suggests that Ti is naturally present in both sedimentary systems.

However, in the case of P, its concentrations were about one order of magnitude higher than those obtained for the Piedras River, except in the three deepest samples. This is due to the influence of the industrial production of phosphoric acid that began around the year 1965 in the surroundings of Huelva city. In this case, the pollution is caused indirectly, as P is dissolved in the phosphogypsum leachates (PGL), since PG was pumped into the Odiel Channel suspended in seawater (20% of PG + 80% of seawater), with P being mainly in dissolution due to its very high solubility in acidic water (pH = 1–2) (Guerrero et al., 2019). Thus, P can be used as a very good tracer/marker of the pollution coming from the phosphogypsum stockpiles and the releases of the phosphoric acid

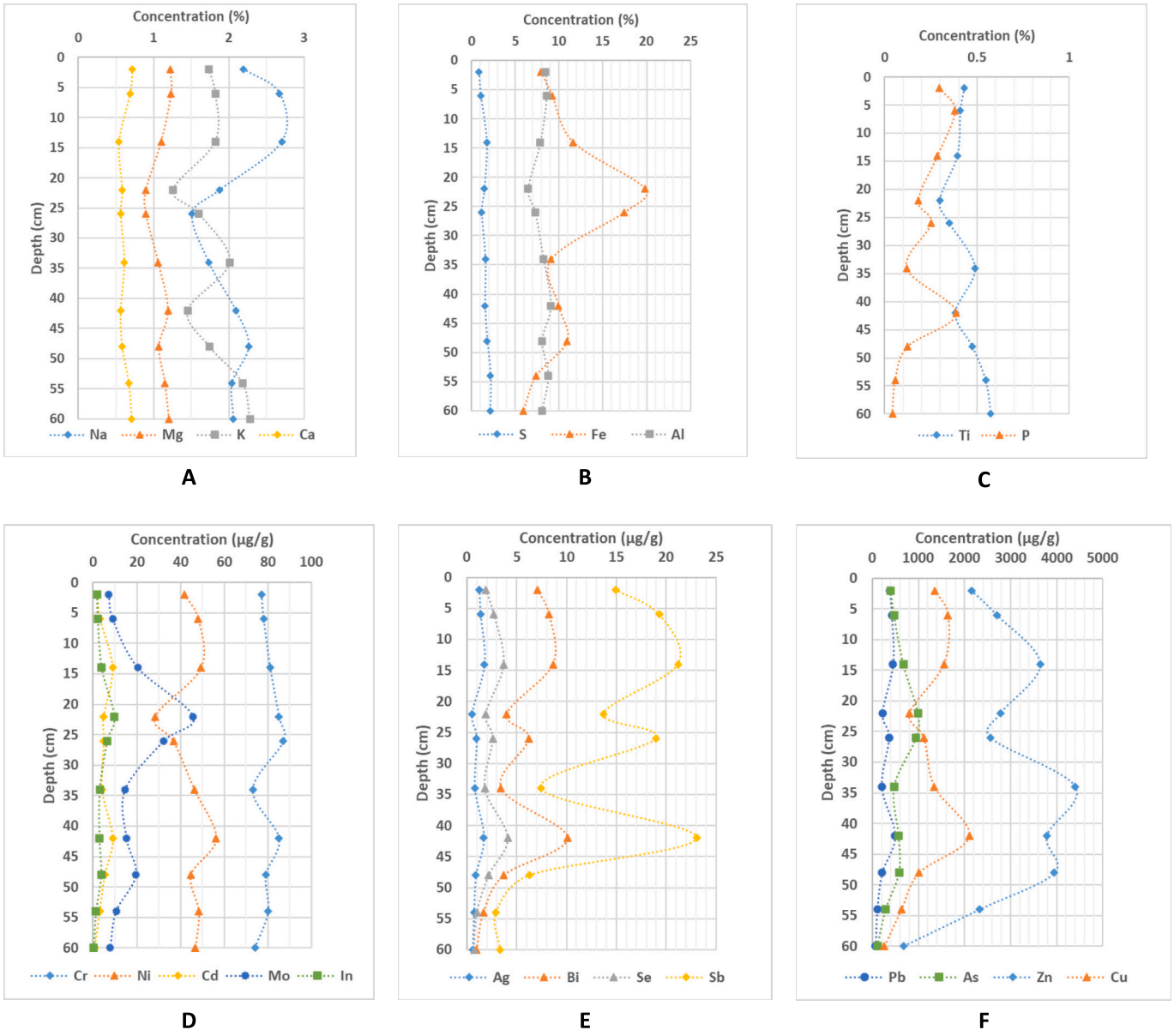


**Fig. 5.** Concentrations of major (from A to C) and trace (from D to F) elements present in the core taken from Bacuta Island.

plants. In Fig. 5c, a significant increase of P concentration at up to 45 cm in depth is observed, demonstrating the impact of the phosphoric acid plants and PG leachates in this area, and enabling the association of the maximum P concentration at about 44 cm with the beginning of the production of phosphoric acid, that is, about the year 1965.

Regarding the trace elements (Fig. 5d, e and f), the same stable elements as those studied in Section 3.1.2 were analyzed. For Cr, Ni, Cd, Mo and In (Fig. 5d), similar concentrations were obtained with respect to those observed in the Piedras River (see Fig. 2d). However, in the case of the Bacuta Island core, maximum concentrations for these elements were generally obtained at 14 cm, 22 cm and 42 cm of depth. This agrees well with the granulometric results (see Fig. A.5b), where the pollution level seems to increase as the percentage of fine fraction (clay + silt) increases, finding maximum values of the fine fraction at 16 cm, 26 cm and 42 cm.

For Ag, Bi, Se and Sb (Fig. 5e), the concentrations were about one order of magnitude higher than those found in the Piedras River (see Fig. 2e). In addition, their behaviors are very similar among them, and they are also similar to that obtained for P. This suggests that these four elements can be provided by PGL.

With regard to Pb, As, Zn and Cu (Fig. 5f), their concentrations were about one order of magnitude higher than those obtained for the Piedras River (see Fig. 2f). The behavior of Pb was similar to that of P, finding three maximum values (at 14 cm, 26 cm and 42 cm). This means that Pb may come from releases of phosphogypsum stockpiles. For the rest of elements, As, Zn and Cu, their relatively high concentrations can be partially due to the AMD influence, which is consistent, since they are toxic elements usually present in massive polymetallic sulphurs. In this case, this is especially true for As, whose behavior was very similar to that of Fe (Fig. 5b).

However, the concentrations of all elements decreased significantly at the greatest depths (>55 cm). This is consistent, since the layers at those depths may have been formed before the mining activity started, that is, before the second half of XIX century. Therefore, the concentrations of all elements tend to be similar to those obtained for unpolluted soils (Rudnick and Gao, 2003).

### 3.2.3. *Concentrations of natural radionuclides*

With respect to the behaviors and activity concentrations of the natural radionuclides along the core taken from Bacuta Island, Fig. 6 shows the concentrations of the radionuclides belonging to the $^{238}$U-series ($^{238}$U, $^{226}$Ra and $^{210}$Pb) (Fig. 6a), $^{232}$Th-series ($^{228}$Ra and $^{228}$Th) and $^{40}$K (Fig. 6b). In addition, these concentrations of radionuclides can be consulted in Table A.6 (Supplementary Material – Appendix A). As can be seen in Fig. 6a, the $^{238}$U concentration pattern is similar to that previously found for P (see Fig. 5c), which is ratified in the next section by the high correlation coefficient between both elements (U *vs* P). This is consistent, since the U also comes from the phosphoric acid industry and PG stockpiles and, given that P and U are very mobile elements, they must follow a very similar behavior/pattern. On the contrary, both $^{226}$Ra and $^{210}$Pb also come from the phosphoric acid industry, but they are very reactive, i.e., they tend to be bound to the particulate material, and they also followed a similar pattern along the core. In addition, the activity concentrations of $^{238}$U, $^{226}$Ra and $^{210}$Pb were much higher than those obtained for the Piedras River, indicating that Bacuta Island is significantly affected by PGL.

For $^{232}$Th-series ($^{228}$Ra and $^{228}$Th) and $^{40}$K (Fig. 6b), their concentrations were very uniform along the core (around 30 Bq kg$^{-1}$), and similar to those found for typical soils (UNSCEAR, 2000). This is consistent, since, in this case, no pollution sources for Th-series radionuclides are affecting this area, thus they are naturally present in this sedimentary system. The $^{232}$Th activity concentration can be calculated from the Th ICP-MS measurements and the relation $^{232}$Th (Bq kg$^{-1}$) = 4.05 Th (mg/kg), finding and average of 38 Bq kg$^{-1}$, which is very similar to that of $^{228}$Ra; therefore, $^{232}$Th-series radionuclides are in secular equilibrium, as is expected in unperturbed estuarine sediments.

In the case of the Bacuta Island core, due to the clear anthropogenic impact, it was necessary to apply the methodology developed by San

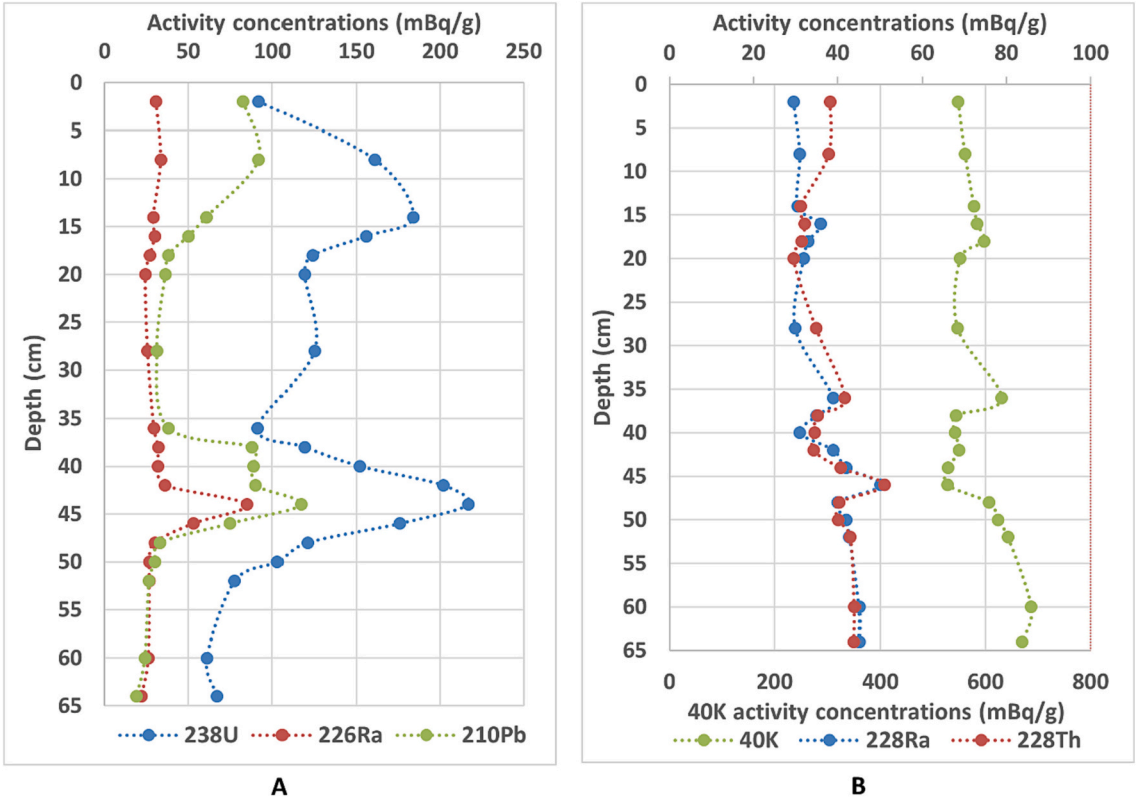


**Fig. 6.** Concentrations of radionuclides, belonging to the $^{238}$U-series (A), and to the $^{232}$Th-series and $^{40}$K (B), present in the core taken from Bacuta Island.

Miguel et al. (2001), where the $^{230}Th/^{232}Th$ activity ratio was previously calculated and plotted against depth (see Fig. A.9 in Supplementary Material – Appendix A), in order to decide in which depth interval it is possible to apply the $^{210}Pb$ dating method. Thus, to make use of the $^{210}Pb$ dating method, the $^{230}Th/^{232}Th$ activity ratio needs to be about 1, in order to avoid possible additional contributions of $^{210}Pb$, which can prevent the proper calculation of unsupported $^{210}Pb$ using the equation: $a$(unsupported $^{210}Pb$) = $a$(supported $^{210}Pb$) – $a$($^{226}Ra$), where $a$(unsupported $^{210}Pb$), $a$(supported $^{210}Pb$) and $a$($^{226}Ra$) are the concentrations of unsupported $^{210}Pb$, supported $^{210}Pb$ and $^{226}Ra$, respectively. Consequently, as can be seen in Fig. A.9, the $^{230}Th/^{232}Th$ activity ratio was stable and about 1 from depths >50 cm. Therefore, since the concentrations of unsupported $^{210}Pb$ are very low from depths >50 cm, it was not possible to apply the $^{210}Pb$ dating method in the case of the Bacuta Island core. However, since the $^{230}Th/^{232}Th$ activity ratio behavior was very similar to the behavior found for the vertical profile of $^{238}U$ concentrations (Fig. 6a), it was possible to further corroborate that the depth of about 44 cm corresponds to the beginning of the industrial activity of phosphoric acid production in Huelva, that is, the year 1965. Consequently, for the polluted part of the Bacuta Island core, it was possible to establish a sedimentation rate of about 0.8 cm $yr^{-1}$.

### 3.2.4. Pollution indexes

Once the concentrations of all stable elements and radionuclides of interest were determined in the case of the Bacuta Island core, and the sedimentary background was properly established (by considering the two deepest layers of our Piedras River core, see Table 1), it was possible to calculate the different pollution indexes, in order to assess the environmental impact in the Bacuta Island.

Regarding the *EF* for major elements, as can be seen in Figs. A.6a and A.6b (see Supplementary Material – Appendix A), the *EF* values for Na, Mg, K, Ca and Ti were below 2, proving that there is no pollution associated with these major elements, and that they are naturally present in the Bacuta Island. In addition, for S, *EF* was also below 2 along the sediment core. However, this does not mean that there is no pollution related to the mining of poly-sulphide minerals from the basins of the Odiel and Tinto Rivers. Due to the fact that sulphur travels in dissolution as sulphate anion ($SO4^{2-}$), this anion is very conservative during the mixing of the fluvial waters and seawater, and, therefore, it does not precipitate during the mixing of these waters, and it finally goes into the Atlantic Ocean, although the majority of Fe precipitates during the waters' mixing process (Nieto et al., 2007; Hierro et al., 2013; Nieto et al., 2013). For P and Fe (Fig. A.6c), the great majority of *EF* values were above 2, which was especially true for P. This is consistent, since affections due to PGL and AMD are significantly present in Bacuta Island, where P and Fe are the main tracers of these pollution sources, respectively.

With regard to the *CF* for the previously analyzed major elements (Figs. A.6d, A.6e and A.6f), it is possible to observe that results analogous to those related to *EF* were obtained, where significant affection was mainly found for P and Fe (*CF* = 2–21 and *CF* = 2–9, respectively), which corresponds to the pollution sources of PGL and AMD, respectively.

With respect to the *EF* for trace elements (Fig. 7a, b and c), for Ag, Se, Bi and Sb (Fig. 7a), the *EF* values were higher than 5 for all these elements at depths lower than 48 cm. The fact of obtaining relatively high *EF* values for these four elements is consistent, since they are mainly provided by PGL, as previously proven (Section 3.2.2). Therefore, given that the industrial production of phosphoric acid began in 1965, for depths greater than about 50 cm, there is no significant contribution of this type of pollution source. In the case of In, Mo, As and Zn (Fig. 7b), they are mainly contributed by AMD, obtaining *EF* values above 10 for all these elements at any depth, except for surface sediments (0–5 cm of depth) and for the deepest sediments (55–60 cm of depth). For Pb, Cu, Cd, Cr and Ni, the *EF* values were higher than 10, except for Cr and Ni, for which *EFs* were close to 1 along the entire core, and at the deepest layers, where the *EF* for Pb, Cu and Cd decreased significantly.

In the case of the *CF* for trace elements (see Figs. A.6 g, A.6 h and A.6i in Supplementary Material – Appendix A), results analogous to those found for *EF* were obtained, where all *CFs* were generally higher than 5 for all the elements, except for Cr and Ni, for which *CFs* were very stable and about 1.5 and 2–4, respectively, for the entire core. Furthermore, at the deepest sediments, that is, about 60 cm of depth, *CF* was generally $\lesssim$ 3; therefore, the pollution was moderate only at about that depth.

With respect to the elements of interest from a toxicological point of view, that is, the heavy metals and As, the "potential ecological risk" index (*PER*) was assessed for each element along the core. As can be seen in Fig. A.7 (see Supplementary Material – Appendix A), all the *PER* values were below 40 (*PER* < 40, that is, low pollution), except for As and Cd, being especially high for Cd, as Cd and As are mainly generated by PGL and AMD, respectively.

When the *PT* and *CD* indexes were calculated for the different samples of the core (Fig. 7d and e, respectively), they were expected to follow the same pattern as Cd, since their toxicity factor ($T_i$) is much higher than that for the rest of toxic elements. Thus, when using the *PT* index (see Table A.1), "serious" (300 ≤ *PT* < 600) and "very serious" (*PT* ≥ 600) ecological risks were observed for all the depths, except for the deepest one, that is, at 60 cm, where the pollution was low. Then, when using the *CD* index (see also Table A.1), a "high degree of pollution" was found for all depths, except for depth ≥ 55 cm, for which the pollution was moderate.

In addition, the *EF* index was also assessed for natural radionuclides in the case of the core taken from Bacuta Island (Fig. 7f and g), as well as the *CF* index (see Figs. A.6j and A.6 k in Supplementary Material – Appendix A). For the radionuclides belonging to the $^{238}U$-series, the *CF* ranged from 2 to 6 for $^{238}U$, while for $^{210}Pb$, the *CF* also reached a maximum of about 6, although values lower than those obtained for $^{238}U$ were detected for the great majority of depths (Fig. A.6j). This is consistent, since the mobility of $^{210}Pb$ is much lower than that of $^{238}U$. The *CF* for $^{226}Ra$ was generally ≤ 2, except at 44 cm, which is logical, since the mobility of $^{226}Ra$ is lower than that of $^{210}Pb$. In addition, the behavior of the *CF* index is in agreement with that resulting from the activity concentrations analyzed in Section 3.2.3 (Fig. 6), as expected, finding maximum values of *CF* at 10–14 cm, 28 cm and 44 cm. In the case of $^{232}Th$-series ($^{228}Ra$ and $^{228}Th$) and $^{40}K$ (Fig. A.6 k), *CF* ranged from 1 to 1.5, that is, no pollution was found due to these radionuclides, indicating that they are naturally present in this sedimentary system. Regarding the *EF* index (Fig. 7f and g), the *EF* was higher than 2 only for $^{238}U$ at 14 cm and 44 cm of depth, and for $^{210}Pb$ at 44 cm. Lastly, for $^{232}Th$-series and $^{40}K$, the *EF* was <2 for the entire core, which is consistent with the *CF* values previously obtained for these radionuclides.

### 3.2.5. Correlation analysis and pollution sources

This Section analyzes the different pollution sources using the correlations between the different major and trace elements. Thus, according to the criteria mentioned in Section 3.1.5, several cases of high correlations were shown in Fig. A.8 (Supplementary Material – Appendix A). In the case of the Mg—Fe pair, the correlation was negative, which is in disagreement with that found for the Piedras River (see Section 3.1.5); this could be due to different basic mechanisms. Therefore, given that Mg is naturally present in Bacuta Island, this means that Fe is being contributed anthropically, with AMD being the pollution source in this case. With regard to Th, as was shown in Sections 3.2.3 and 3.2.4, the presence of Th is natural. Since the relationship between Th and Fe is negative, it further corroborates that Fe comes from AMD contribution. Lastly, in regard with As—Fe, given that Fe is the tracer of AMD, and their correlation is positive, it suggests that As comes mainly from the contribution of a pollution source, which is AMD in this case, as is shown in Section 3.2.2 (Fig. 5).

On the contrary, in the case of P, it is possible to observe that U, Bi and Pb have positive and linear correlations, but they have no significant

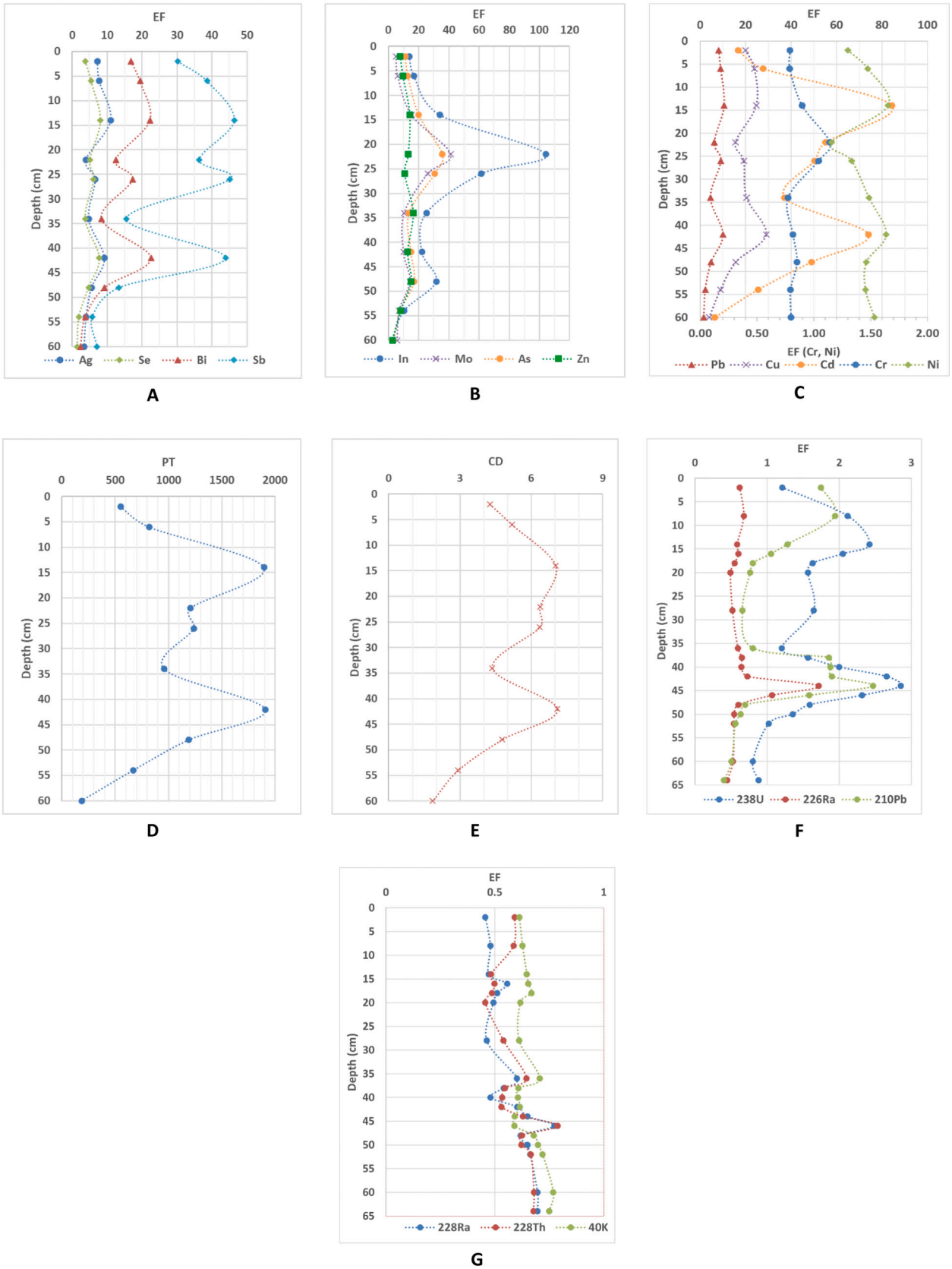


**Fig. 7.** Enrichment factor (*EF*) (from A to C), potential toxicity (*PT*) (D) and contamination degree (*CD*) (E) obtained for the trace elements in the case of the core taken from Bacuta Island, where *EF* was calculated in relation to the two deepest samples of the core taken from the Piedras estuary (see Table 1), considering Al as the normalizer element for the *EF* calculations. The *EF* was also obtained for radionuclides (F and G).

correlations with Fe (see correlation matrix in Supplementary Material – Appendix B). This demonstrates that these three elements come mainly from the fertilizer plant activities, since P is considered as the tracer of pollution coming from this industry.

Supplementary Material – Appendix B shows the Principal Component Analysis (PCA) carried out for Bacuta Island. In the biplot of the principal components F1 and F2, the positive axis of F1 can be identified as the affection coming from the fertilizer industry, since P can be found in this axis, while Fe can be found in the positive axis of F2, thus this axis represents the influence of AMD. Therefore, in the positive axis of F1, it is possible to find elements such as U, Bi and Pb, while in the positive axis of F2, As is present. This corroborates the analysis previously carried out to find the pollution sources for these four elements.

Finally, the correlation between Fe and P was found to be not significant (see Supplementary Material), since these two elements come from different pollution sources in the case of the Bacuta Island, as previously demonstrated (AMD and fertilizer industry, respectively). This behavior is the opposite of that found for the Piedras River (see Section 3.1.5), which is consistent.

## 4. Conclusions

An assessment of the environmental impact exiting in the estuarine biosphere reserve in Southwestern Iberian Peninsula was carried out. To this end, a suitable sedimentary background was assessed and established for the evaluation of the affection in this biosphere reserve generated by the fertilizer complex located in the Huelva estuary, that is, between the Tinto and Odiel Rivers.

The following main conclusions were drawn from this study:

1. The enrichment factor (*EF*) and contamination factor (*CF*) were calculated for heavy metals and natural radionuclides in the case of the Piedras River, achieving *EF* and *CF* values very close to 1 for all cases. This proves that the Piedras River is a proper sedimentary background in our case.
2. Regarding the core taken from both the Piedras estuary and Bacuta Island, it was possible to observe that clay and silt were the predominant granulometric fractions for both ecosystems. This fact demonstrates that the Piedras estuary is a good reference area for the Odiel estuary, finding a maximum percentage of clay + silt of about 90%.
3. P and Fe were the elements with outstanding concentrations, observing a clear indirect affection of phosphogypsum stockpiles by means of their leachates (PGL), and the impact of acid mine drainage (AMD). Thus, P and Fe were suitable for tracing the pollution coming from PGL and AMD, respectively.
4. The concentrations of several trace elements such as Bi, Pb, Se and Sb were much higher (about 1 order of magnitude) than those obtained for the Piedras River. These elements followed a very similar behavior as that followed by P; therefore they were mainly contributed by PGL. For As, Cu and Zn, concentrations of about 1 order of magnitude higher than those found for the Piedras River were also obtained, where the main pollution source for these elements was AMD, since their behaviors were similar to that of Fe.
5. In the case of radionuclides belonging to the $^{238}$U-series, a clear impact by PGL was observed, and not from AMD. For radionuclides belonging to the $^{232}$Th-series and $^{40}$K, very stable concentrations were found along the entire core, and they were similar to those related to unpolluted soils.
6. The pollution indexes (*EF* and *CF*) and the potential ecological risk (*PER*) reached values of serious and very serious pollution in Bacuta Island for most of the trace elements, as well as Fe and P, although it was observed that, in the deepest sediments (>50 cm depth), the pollution was much less significant, showing moderate values. This dependence of pollution on depth was observed using the potential toxicity (*PT*) and the contamination degree (*CD*). Lastly, *EF* and *CF* were used for natural radionuclides, observing low-moderate pollution for radionuclides belonging to the $^{238}$U-series, and no pollution in the case of the $^{232}$Th-series and $^{40}$K.

## CRediT authorship contribution statement

**A. Barba-Lobo:** Conceptualization, Data curation, Formal analysis, Investigation, Methodology, Validation, Writing – original draft, Writing – review & editing. **B. García-González:** Data curation. **J.L. Guerrero:** Writing – original draft, Writing – review & editing. **J.P. Bolívar:** Conceptualization, Investigation, Methodology, Writing – original draft, Writing – review & editing.

## Declaration of competing interest

The authors declare that they have no known competing financial interests or personal relationships that could have appeared to influence the work reported in this paper.

## Data availability

Data will be made available on request.

## Acknowledgments

This research was partially funded by the University of Huelva and the Operative FEDER Program-Andalusia 2014-2020 (UHU-1255876, UHU-202020); The European Regional Development Fund through the Spanish Ministry of Science, Innovation and Universities' Research Agency (research grants PID2020-116461RB-C21 and 116461RA-C22); and the Andalusian government (I + D + i-JAPAIDI-Retos, project Ref.: PY20_00096, and Diagnosis and proposals for the environmental recovery of areas affected by industrial and mining activities; Implications for the Huelva estuary (RESTOREHU), Ref.: TED2021-130361B-I00). José Luis Guerrero thanks the Spanish Ministry of Universities for the Margarita Salas research grant.

## Appendix A. Supplementary data

Supplementary data to this article can be found online at https://doi.org/10.1016/j.marpolbul.2024.116225.

## References

Aduvire, O., 2006. Drenaje ácido de mina generación y tratamiento. Dirección de Recursos Minerales y Geoambiente, Instituto Geológico y Minero de España, Madrid (140 pp.).

Barba-Lobo, A., San Miguel, E.G., Lozano, R.L., Bolívar, J.P., 2021a. A general methodology to determine natural radionuclides by well-type HPGe detectors. Measurement 181, 109561. https://doi.org/10.1016/j.measurement.2021.109561.

Barba-Lobo, A., Mosqueda, F., Bolívar, J.P., 2021b. An upgraded Lab-based method to determine natural γ-ray emitters in NORM samples by using Ge detectors. Measurement 186, 110153. https://doi.org/10.1016/j.measurement.2021.110153.

Bolívar, J.P., García-Tenorio, R., Garcia-Leon, M., 1995. Enhancement of natural radioactivity in soils and saltmarshes surrounding a non-nuclear industrial complex. Sci. Total Environ. 173, 125–136.

Bolívar, J.P., García Tenorio, R., Matarranz, M., J. L., 2008. Evaluación radiológica del apilamiento de fosfoyesos de las marismas del río Tinto (Huelva).

Bolívar, J.P., Martín, J.E., García-Tenorio, R., Pérez-Moreno, J.P., Mas, J.L., 2009. Behaviour and fluxes of natural radionuclides in the production process of a phosphoric acid plant. Appl. Radiat. Isot. 67 (2), 345–356. https://doi.org/10.1016/j.apradiso.2008.10.012.

Borrego, J., Morales, J.A., De la Torre, M.L., Grande, J.A., 2002. Geochemical characteristics of heavy metal pollution in surface sediments of the Tinto and Odiel river estuary (southwestern Spain). Environ. Geol. 41 (7), 785–796. https://doi.org/10.1007/s00254-001-0445-3.

Caliani, J.C., Ruíz, F., Galán, E., 1997. Clay mineral and heavy metal distributions in the lower estuary of Huelva and adjacent Atlantic shelf, SW Spain. Sci. Total Environ. 198, 181–200. https://doi.org/10.1016/S0048-9697(97)05450-8.

Curcio, A.C., Barbero, L., Casas-Ruiz, M., López-Ramírez, J.A., 2019. Fractionation of U and heavy metals into the colloidal fraction in acid mine drainage conditions in the

Río Tinto area (SW Spain). J. Contam. Hydrol. 222, 65–75. https://doi.org/10.1016/j.jconhyd.2019.02.008.
Delgado, J., Boski, T., Nieto, J.M., Pereira, L., Moura, D., Gomes, A., Sousa, C., García-Tenorio, R., 2012. Sea-level rise and anthropogenic activities recorded in the late Pleistocene/Holocene sedimentary infill of the Guadiana Estuary (SW Iberia). Quat. Sci. Rev. 33, 121–141. https://doi.org/10.1016/j.quascirev.2011.12.002.
Díaz-Asencio, M., Corcho Alvarado, J.A., Alonso-Hernández, C., Quejido-Cabezas, A., Ruíz-Fernández, A.C., Sánchez-Sánchez, M., Gómez-Mancebo, M.B., Froidevaux, P., Sánchez-Cabeza, J.A., 2011. Reconstruction of metal pollution and recent sedimentation processes in Havana Bay (Cuba): a tool for coastal ecosystem management. J. Hazard. Mater. 196, 402–411. https://doi.org/10.1016/j.jhazmat.2011.09.037.
García-Tenorio, R., García-León, M., 1996. Radioactive impact of some phosphogypsum piles in soils and salt marshes evaluated by γ-ray spectrometry. Appl. Radiat. Isot. 47 (9–10), 1069–1075.
Gázquez, M.J., Bolívar, J.P., García-Tenorio, R., Galán, F., 2009. Natural occurring radionuclide waste in spain: the Huelva phosphogypsum stacks case. In: 1st Spanish National Conference on Advances in Materials Recycling and Eco – Energy. Madrid, 12-13 November 2009, pp. 75–78.
Gözel, F., Belivermis, M., Sezer, N., Kurt, M.A., Sikdokur, E., Kilic, Ö., 2022. Chronology of trace elements and radionuclides using sediment cores in Golden Horn Estuary, Sea of Marmara. Environ. Pollut. 315, 120359 https://doi.org/10.1016/j.envpol.2022.120359.
Guerrero, J.L., Gutiérrez-Álvarez, I., Mosqueda, F., Olías, M., García-Tenorio, R., Bolívar, J.P., 2019. Pollution evaluation on the salt-marshes under the phosphogypsum stacks of Huelva due to deep leachates. Chemosphere 230, 219–229. https://doi.org/10.1016/j.chemosphere.2019.04.212.
Guerrero, J.L., Gutiérrez-Álvarez, I., Hierro, A., Pérez-Moreno, S.M., Olías, M., Bolívar, J. P., 2021a. Seasonal evolution of natural radionuclides in two rivers affected by acid mine drainage and phosphogypsum pollution. Catena 197, 104978. https://doi.org/10.1016/j.catena.2020.104978.
Guerrero, J.L., Pérez-Moreno, S.M., Gutiérrez-Álvarez, I., Gázquez, M.J., Bolívar, J.P., 2021b. Behaviour of heavy metals and natural radionuclides in the mixing of phosphogypsum leachates with seawater. Environ. Pollut., 115843 https://doi.org/10.1016/j.envpol.2020.115843.
Hakason, L., 1979. An ecological risk index for aquatic pollution control. A sedimentological approach. In: Water Research (Vol. 14).
Hierro, A., Bolívar, J.P., Vaca, F., Borrego, J., 2012. Behavior of natural radionuclides in surficial sediments from an estuary impacted by acid mine discharge and industrial effluents in Southwest Spain. J. Environ. Radioact. 110, 13–23.
Hierro, A., Martín, J.E., Olías, M., García, C., Bolívar, J.P., 2013. Uranium behavior during a tidal cycle in an estuarine system affected by acid mine drainage (AMD). Chem. Geol. 342, 110–118.
Kerolli-Mustafa, M., Fajković, H., Ronèević, S., Ćurković, L., 2015. Assessment of metal risks from different depths of jarosite tailing waste of Trepça Zinc Industry, Kosovo based on BCR procedure. J. Geochem. Explor. 148, 161–168. https://doi.org/10.1016/j.gexplo.2014.09.001.
Lario, J., Alonso-Azcárate, J., Spencer, C., Zazo, C., Goy, J.L., Cabero, A., Dabrio, C.J., Borja, F., Borja, C., Civis, J., García-Ródriguez, M., 2016. Evolution of the pollution in the Piedras River Natural Site (Gulf of Cadiz, southern Spain) during the Holocene. Environ. Earth Sci. 75 (6) https://doi.org/10.1007/s12665-016-5344-8.
Le Gall, M., Ayrault, S., Evrard, O., Laceby, J.P., Gateuille, D., Lefèvre, I., Mouchel, J.-M., Meybeck, M., 2018. Investigating the metal contamination of sediment transported by the 2016 Seine River flood (Paris, France). Environ. Pollut. 240, 125–139. https://doi.org/10.1016/j.envpol.2018.04.082.
Lee, P.-K., Lim, J., Jeong, Y.-J., Hwang, S., Lee, J.-Y., Choi, B.-Y., 2021. Recent pollution and source identification of metal(loid)s in a sediment core from Gunsan Reservoir, South Korea. J. Hazard. Mater. 416, 126204 https://doi.org/10.1016/j.jhazmat.2021.126204.
Liu, J., Deng, S., Liu, M., Liu, G., Li, C., 2021. Distribution of heavy metals and radionuclides in the sediments and their environmental impacts in Nansha Sea area, South China Sea. Mar. Pollut. Bull. 166, 112192 https://doi.org/10.1016/j.marpolbul.2021.112192.
Luo, M., Kang, X., Liu, Q., Yu, H., Tao, Y., Wang, H., Niu, Y., Niu, Y., 2022. Research on the geochemical background values and evolution rules of lake sediments for heavy metals and nutrients in the eastern China Plain from 1937 to 2017. J. Hazard. Mater. 436, 129136 https://doi.org/10.1016/j.jhazmat.2022.129136.
Morillo, J., Usero, J., Gracia, I., 2004. Heavy metal distribution in marine sediments from the southwest coast of Spain. Chemosphere 55 (3), 431–442. https://doi.org/10.1016/j.chemosphere.2003.10.047.
Mujica, B., Aurelio, J., Macías, P., 2008. macla. nº 10. noviembre'08 revista de la sociedad española de mineralogía.
Nieto, J.M., Sarmiento, A.M., Olías, M., Cánovas, C.R., Riba, I., Kalman, J., Delvalls, T.A., 2007. Acid mine drainage pollution in the Tinto and Odiel rivers (Iberian Pyrite Belt, SW Spain) and bioavailability of the transported metals to the Huelva estuary. Environ. Int. 33, 445–455. https://doi.org/10.1016/j.envint.2006.11.010.
Nieto, J.M., Sarmiento, A.M., Canovas, C.R., Olias, M., Ayora, C., 2013. Acid mine drainage in the Iberian Pyrite Belt: 1. Hydrochemical characteristics and pollutant load of the Tinto and Odiel rivers. Environ. Sci. Pollut. Res. 20 (11), 7509–7519. https://doi.org/10.1007/s11356-013-1634-9.
Olías, M., Cánovas, C.R., Nieto, J.M., Sarmiento, A.M., 2006. Evaluation of the dissolved contaminant load transported by the Tinto and Odiel rivers (South West Spain). Appl. Geochem. 21, 1733–1749. https://doi.org/10.1016/j.apgeochem.2006.05.009.
Papaslioti, E.M., Pérez-López, R., Parviainen, A., Sarmiento, A.M., Nieto, J.M., Marchesi, C., Delgado-Huertas, A., Garrido, C.J., 2018. Effects of seawater mixing on the mobility of trace elements in acid phosphogypsum leachates. Mar. Pollut. Bull. 127, 695–703. https://doi.org/10.1016/j.marpolbul.2018.01.001.
Pérez-López, R., Nieto, J.M., López-Cascajosa, M.J., Díaz-Blanco, M.J., Sarmiento, A.M., Oliveira, V., Sánchez-Rodas, D., 2011. Evaluation of heavy metals and arsenic speciation discharged by the industrial activity on the Tinto-Odiel estuary, SW Spain. Mar. Pollut. Bull. 62 (2), 405–411. https://doi.org/10.1016/j.marpolbul.2010.12.013.
Pérez-López, R., Macías, F., Cánovas, C.R., Sarmiento, A.M., Pérez-Moreno, S.M., 2016. Pollutant flows from a phosphogypsum disposal area to an estuarine environment: an insight from geochemical signatures. Sci. Total Environ. 553, 42–51. https://doi.org/10.1016/j.scitotenv.2016.02.070.
Riba, I., Delvalls, T.A., Forja, J.M., Gómez-Parra, A., 2002. Evaluating the heavy metal contamination in sediments from the Guadalquivir estuary after the Aznalcóllar mining spill (SW Spain): a multivariate analysis approach. Environ. Monit. Assess. 77 (2), 191–207. https://doi.org/10.1023/A:1015828020313.
Royal Decree, 2005. Real Decreto 9/2005, de 14 de Enero, por el que se establece la relación de actividades potencialmente contaminantes del suelo y los criterios y estándares para la declaración de suelos contaminados.
Rudnick, R.L., Gao, S., 2003. The composition of the continental crust. In: Holland, H.D., Turekian, K.K. (Eds.), Treatise on Geochemistry, Vol. 3. The Crust, Elsevier-Pergamon, Oxford, pp. 1–64. https://doi.org/10.1016/b0-08-043751-6/03016-4.
Sáez, R., Pascual, E., Toscano, M., Almodóvar, G.R., 1999. The Iberian type of volcano–sedimentary massive sulphide deposits. Mineral. Deposita 34, 549–570. https://doi.org/10.1007/s001260050220.
San Miguel, E.G., Bolívar, J.P., García-Tenorio, R., Martín, J.E., 2001. 230Th/232Th activity ratios as a chronological marker complementing 210Pb dating in an estuarine system affected by industrial releases. Environ. Pollut. 112, 361–368. https://doi.org/10.1016/s0269-7491(00)00146-9.
Sousa, C.A.M., Delgado, J., Szalaj, D., Boski, T., 2019. Holocene background concentrations and actual enrichment factors of metals in sediments from Ria Formosa, Portugal. Mar. Pollut. Bull. 149 https://doi.org/10.1016/j.marpolbul.2019.110533.
UNSCEAR, 2000. Sources and Effects of Ionizing Radiation United Nations Scientific Committee on the Effects of Atomic Radiation UNSCEAR 2000 Report to the General Assembly, with Scientific Annexes Volume I: Sources United Nations.
Vineethkumar, V., Sayooj, V.V., Shimod, K.P., Prakash, V., 2020. Estimation of pollution indices and hazard evaluation from trace elements concentration in coastal sediments of Kerala, southwest Coast of India. Bull. Natl. Res. Cent. 44 (1) https://doi.org/10.1186/s42269-020-00455-0.
Yushin, N., Jakhu, R., Chaligava, O., Grozdov, D., Zinicovscaia, I., 2023. Natural and anthropogenic radionuclides concentration with heavy metals analysis of the sediments collected around Novaya Zemlya. Mar. Pollut. Bull. 194, 2023. https://doi.org/10.1016/j.marpolbul.2023.115346.
Zhang, R., Guan, M., Shu, Y., Shen, L., Chen, X., Zhang, F., Li, T., 2016. Historical record of lead accumulation and source in the tidal flat of Haizhou Bay, Yellow Sea: insights from lead isotopes. Mar. Pollut. Bull. 106, 383–387. https://doi.org/10.1016/j.marpolbul.2016.02.046.